JOURNAL OF AIRCRAFT
Vol. 40, No. 3, May–June 2003

Evaluation of the Wright 1901 Glider Using Full-Scale Wind-Tunnel Data

Kevin Kochersberger*
Rochester Institute of Technology, Rochester, New York 14623
Robert Ash,† Colin Britcher,† and Drew Landman‡
Old Dominion University, Norfolk, Virginia 23529
and
Ken Hyde§
The Wright Experience, Warrenton, Virginia 20188

A reproduction of the Wright 1901 glider, built by The Wright Experience™ in Warrenton, Virginia, was wind-tunnel tested at the Langley Full Scale Tunnel through a range of conditions similar to those experienced in flight 100 years earlier. The testing included a range of dynamic pressures that encompassed the stall and maximum gliding speeds, angles of attack of up to 20 deg, and sideslip angles of up to 15 deg. The results of the test were used to determine not only lift, drag, and moment coefficients, but also control power from the actuation of the canard and wing warping controls. A maximum lift/drag ratio of 3.9 was recorded for an untreated cloth condition. When the cloth was "airproofed" and ground effect considered, the optimal lift/drag increased to 5.8. This compares favorably with the measurements and observations made by the Wrights, reporting optimal lift/drag values of around 6.

Nomenclature

b	=	wingspan
C_D	=	drag coefficient
C_L	=	lift coefficient
C_{Lo}	=	lift coefficient intercept
$C_{L\alpha}$	=	lift curve slope
C_l	=	rolling moment coefficient
C_{lp}	=	roll damping
$C_{l\beta}$	=	dihedral effect
$C_{l\delta w}$	=	roll control power
C_m	=	pitching moment coefficient, referenced to to c.g.
$C_{m\alpha}$	=	pitching moment curve slope
$C_{m\delta c}$	=	canard control power
C_n	=	yawing moment coefficient
$C_{n\beta}$	=	yaw stability
C_Y	=	side force coefficient
$\bar{c}$	=	chord
L/D	=	lift/drag ratio
n_z	=	vertical load factor
P_{C_X}	=	Confidence interval of 95%
p, q, r	=	x, y, z roll rates
Q	=	dynamic pressure
u, v, w	=	x, y, z velocities
$x_{\text{c.g.}}$	=	Center of gravity position
$x_{\text{c.p.}}$	=	Center of pressure position
x_{np}	=	Neutral point position
α	=	angle of attack
β	=	sideslip angle
δ_c	=	canard deflection
δ_w	=	warp deflection
ζ	=	damping ratio
θ	=	pitch angle
λ	=	system pole
ϕ	=	roll angle

Received 25 July 2002; revision received 20 January 2003; accepted for publication 26 January 2003.

*Associate Professor, Mechanical Engineering. Member AIAA.
†Professor, Aerospace Engineering. Associate Fellow AIAA.
‡Associate Professor, Aerospace Engineering. Member AIAA.
§President, The Wright Experience. Member AIAA.

Introduction

In retrospect, it may seem unusual that the world's first functional powered aircraft had not been wind-tunnel tested until a few years ago. In 1999, a full-scale 1903 Wright Flyer was evaluated by volunteers from the Los Angeles AIAA Section with the support of the NASA Ames Research Center 40 × 80 tunnel.[1] From Culick's earlier test of a $\frac{1}{6}$ scale model of the Flyer in the Graduate Aerospace Laboratories California Institute of Technology tunnel in 1980 (see Ref. 2) and the $\frac{1}{8}$ scale model test at Northrop Corp. in 1981, a preliminary database of aerodynamic coefficients for the Flyer has emerged. From these coefficients, simulations have been implemented both in ground-based and airborne simulators[3] to evaluate the handling qualities of the aircraft.

With the upcoming Centennial of Flight celebration on 17 December 2003, there has been a renewed interest in modeling the aerodynamics of Wright aircraft to understand how their flight-test experiments influenced their designs. A kite and three pilot-carrying gliders were constructed before the powered machine, and these formed the basis for all theory used in their successful development program. Starting in 1900 and ending in 1902, the gliders progressively became more controllable and more efficient, so that, by the end of 1902, a fully functional, three-axis controlled machine was at hand. Because the gliders were pivotal to the Wrights' success, an aircraft wind-tunnel testing program has been launched at the Langley Full Scale Tunnel in Hampton, Virginia, starting with the 1901 glider. The 1902 glider, the 1911 Model B, and the 1903 Flyer are all scheduled for future testing at the tunnel.

Background

In 1899, the Wright brothers began a flight-test program to answer questions about the stability and control of aircraft. It was their understanding, and to a degree Chanute's understanding several years earlier, that the most vexing problem in flying machine development was how to regulate the glide path and lateral direction of the machine. Using a box with ends cut out, Wilbur Wright intuitively solved the roll control problem when he applied pressure to the

opposite corners of the box, resulting in the warping distortion of the box. This warping subsequently became perhaps the first example of an aircraft subsystem (control) being integrated directly into another subsystem (structures) to minimize weight. The Wrights built a 5-ft (1.5 m) wingspan kite to demonstrate the warping control and found it successful enough to proceed with a full-sized glider.[4]

In October of 1900, a biplane glider designed by the Wrights was kited and test flown in Kitty Hawk, North Carolina with limited success. This glider, with its 17-ft, 5-in. (5.3 m) wingspan, featured a canard (or horizontal "rudder") for pitch control and wing warping for lateral control. Extensive testing was performed with the glider tethered, and measurements of lift and drag were made with a spring scale. Despite its wing area of 165 ft^2 (200 ft^2 were to be used, but restrictions on available lumber size reduced the span), this glider managed to fly piloted on a slope of 9.5 deg for an L/D of around 6. As Wilbur subsequently reported, "... the hours and hours of practice we had hoped to obtain finally dwindled down to about two minutes. ..."[5] The tests of 1900 were complete and the Wrights returned to Dayton to begin work on the 1901 glider.

Although the 1900 machine demonstrated the controllability the Wrights were looking for through the use of the adjustable canard and the wing warping system, they found its lifting performance to be less than predicted. In particular, the angle of attack required for sustained flight was about six times greater than they had predicted, either when the glider was kited or flown piloted.[6] For this reason, the 1901 glider featured an enlarged 285-ft^2 wing, with a 22-ft (6.7 m) wingspan and a 6.5-ft (2.0 m) mean chord. The canard measured 18.7 ft^2. With a 140-lb pilot onboard, the gross weight was 240 lb.

The 1901 design retained the wing warping mechanism that functioned exactly as Wilbur had discovered it with the box model in 1899. A foot-operated T bar changed the length of the fore–aft diagonal support lines in their modified Pratt truss biplane design (the nondeforming version of which Chanute had used in his glider designs). Manipulation of the diagonal support cable lengths effectively warped the wings by moving the diagonal wing endpoints either closer or farther apart. The canard was actuated by two levers pivoted near the leading edge of the bottom main wing, which allowed the operator to control the deflection of the canard while at the same time retaining the ability to move slightly forward or backward to adjust the c.g. The ash ribs in the canard were bowed under the action of the levers, causing the canard airfoil to change its camber, thus providing additional control power over simply pivoting the noncambered control surface. Figure 1 shows the glider flying at Kitty Hawk.

To compensate for the reduced performance found in the 1900 glider, the camber of the wing was increased from $(1/19)\bar{c}$ to $(1/12)\bar{c}$, similar to Lilienthal's design and the basis for the Duchemin–Lilienthal table relating lift, drift (or drag), and angle of attack. This table was considered the definitive source for sizing wings at the time. However, as the Wrights accumulated flight-testing knowledge during their 1900 and 1901 test campaigns, they became convinced that the Duchemin–Lilienthal table was contributing to serious discrepancies between their design estimates and their actual flight results.

Gliding experiments began with the new machine in July 1901 with limited success. In addition to finding that the aircraft lifted less weight at a given angle of attack than predicted (similar to the previous year), the aircraft was difficult to control longitudinally. Culick[7] has concluded that the Wright brothers were unaware of the moment balance equations that would have greatly facilitated their isolation of the root cause of their glider handling problems. However, they understood intuitively (and from measurements) that a forward shift in the c.p. as the angle of attack increased would result in the observed longitudinal control problem. This was confirmed in a kiting flight test of a single 1901 glider wing panel, where the c.g. and the c.p. were measured as a function of angles of attack. The data supported Wilbur's flight-test results that were indicative of a pitch-unstable aircraft.[8]

Deducing correctly that the increased camber caused the unwanted pitching moment change, the Wrights reduced their 1901 glider wing camber by trussing down the centers of the wing panels.[9]

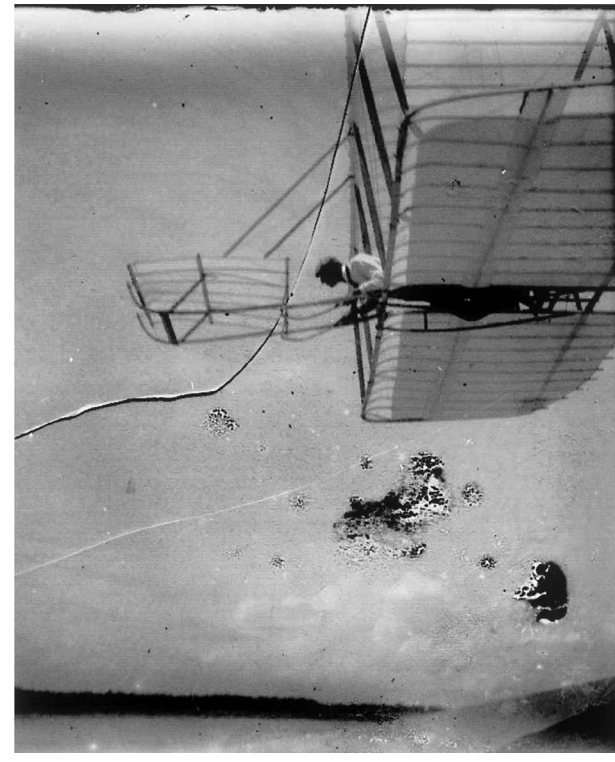

Fig. 1 Glider 1901 in flight.

Not only did this reduce the camber, approximating that used in 1900, but it also added reflex, unknown to the Wrights, but very effective in reducing the pitching moment variation. Commonly found on flying-wing aircraft or aircraft with limited tail volume, reflex provides longitudinal stability by negating the camber-induced moment. When this was accomplished, the increased drag of the trussing wires was a minor penalty to the improved longitudinal controllability. Piloted glider flights of well over 300 ft became commonplace, and the 1901 distance record was 389 ft. Wilbur wrote,[10]

> ... the machine with its new curvature never failed to respond promptly to even small movements of the rudder (canard). The operator could cause it to almost skim the ground, following the undulations of the surface, or he could cause it to sail out almost on a level with the starting point, and, passing high above the foot of the hill, gradually settle down to the ground.

Along with about 100 piloted flights in the 1901 glider, numerous kite flight tests were conducted to measure lift and drag in various wind speeds. A maximum L/D of around 6 was again reported in both the piloted and kited configurations.[9] Angles of attack were recorded that confirmed their belief that the Lilienthal lift and drift (drag) data were in error. These concerns lead them to embark on a true aeronautical research program in Dayton, starting in late 1901, that utilized wind-tunnel testing to optimize the airfoils selected for their wing designs and, subsequently, propellers.[11] In part because of the failures of 1901, the Wrights pursued the science of flight with renewed intensity that led them to the successful first powered flight of 1903.

Overview of Test Configuration

A reproduction of the 1901 Wright glider was fabricated at The Wright Experience™ in Warrenton, Virginia for the purposes of rediscovering the events leading up to the successful first powered flight of 1903. In partnership with NASA Langley Research Center and Old Dominion University (ODU), this aircraft was tested at the Langley Full Scale Tunnel (LFST), operated by ODU since 1997 under a memorandum of agreement with NASA. This facility (formerly the NASA 30×60) is the second largest in the United States in terms of test-section size.

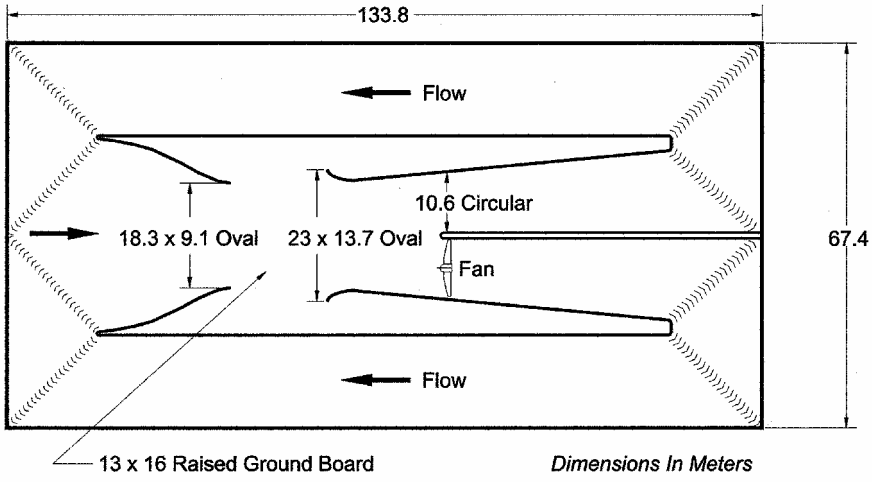

Fig. 2 Overall dimensions of the LFST.

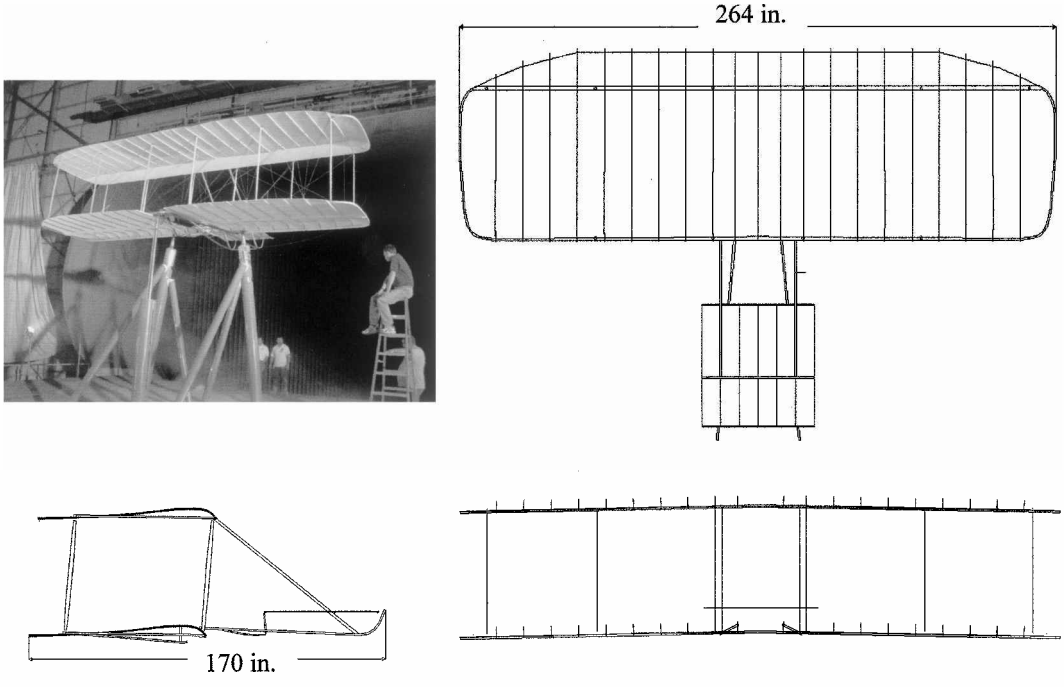

Fig. 3 Dimensions of the 1901 glider.

The open jet test section of the LFST is semi-elliptical in cross section with a width of 18.29 m (60 ft) and a height of 9.14 m (30 ft), as shown in Fig. 2. The elevated ground board is 13 m (42.5 ft) wide by 16 m (52 ft) long and features a turntable with a diameter of 8.7 m (28.5 ft). Power is supplied by two 3-MW (4000-hp) electric motors driving two 11-m- (35.5-ft-) diam four-bladed fans.

Full-scale aircraft are supported on three struts, which are shielded from the flow to minimize tare loads and corrections. The two main struts are used as pivots to allow the aircraft to pitch by articulating the third (tail) strut. This entire assembly is mounted to the turntable and can be rotated in yaw. The struts transfer loads to the six degree-of-freedom external balance located below the turntable. The balance utilizes load reduction linkages consisting of lever arms and knife-edge pivots, ultimately driving balance beam scales with strain gauge outputs. The scale weights are determined using a 16-bit, A/D converter and personal computer based analysis software.

Just before this test, the balance was refurbished and a full calibration performed. All knife-edge pivots were examined and sharpened or replaced as necessary. Individual scale calibrations were established by the use of traceable weight standards. A load frame was then installed on the aircraft support struts, and the balance was loaded and calibrated in all axes, including determination of first-order interactions.[12] The 95% confidence intervals of outputs in balance axes, based on deadweight loadings, can be propagated through the coordinate transformations to aircraft axes, when procedures outlined in Ref. 13 were followed. At a nominal test dynamic pressure of $Q = 2.0$ psf, the 95% confidence intervals of coefficients in aircraft coordinates are estimated to be

$$P_{C_L} = 0.0046, \quad P_{C_D} = 0.0032, \quad P_{C_Y} = 0.006$$
$$P_{C_m} = 0.009, \quad P_{C_l} = 0.003, \quad P_{C_n} = 0.002 \quad (1)$$

The 1901 glider was mounted to the three-post system via the inboard wing strut attachment points on the bottom leading-edge spar and also at the center of the rear spar. Rod-end bearings were used on the rear spar attachment point to allow for the wing warping action to occur. Note that, in free flight, wing warping produces opposite-direction roll between the front and rear spars and opposite direction yaw between the top and bottom wings. Fixing the bottom leading-edge spar in the tunnel test creates a reference datum that should be noted when converting to the in-flight conditions. The angle-of-attack reference was taken to be a line from the nose of the leading edge of the lower wing to the bottom trailing edge of the ribs. Figure 3 shows the glider mounted in the tunnel, with the mounting

Table 1 Test run schedule, 1901 glider

Runs	Warp	Canard	Beta	AOA minimum	AOA maximum	Q, psf
1–6	0	0	0	−2	20	0.85–2.8
7–8	0	$+\frac{1}{2}, -\frac{1}{2}$	0	2	12	1.5
9–17	0	+full, −full	0	0	14	1.0–2.8
18–19	0	0	+15, −15	2	8	2.0
20–21	$+\frac{1}{3}, -\frac{1}{3}$	0	0	2	6	2.5
22–23	$+\frac{2}{3}, -\frac{2}{3}$	0	0	2	11	1.5
24–29	+full, −full	0	0	2	14	1.0–2.4
30–31	−full	0	+8, −8	2	20	1.0
32–35	All zero deflections, fabric airproofed			2	20	0.88–2.0
36	Warp 0, Canard + full, Beta 0, fabric airproofed			2	8	2.0

interface structure sized according to calculated loads obtained, in part, from a model based on vortex lattice theory. All data shown are corrected for support tares (primarily drag).

With an elliptical cross section, the 60-ft tunnel width results in a jet that is somewhat below 60 ft, but is still of the order of 2.5 times the wingspan. The ratio of total wing area (285 ft^2) to flow cross section ($\approx$1600 ft^2) is less favorable, leading to concern over boundary corrections. If upwash interference is cast in the classical form as shown hereafter, then the value of δ can be estimated using arrays of horseshoe vortex images[14]:

$$\Delta\alpha_i = \delta(S/C)C_L \tag{2}$$

It is found that, for this particular case, the value of $\Delta\alpha_i$ is below 0.15 deg for a C_L of unity. This is considered sufficiently small to justify reporting data uncorrected for boundary interference. Note that the sign of corrections for open and closed boundaries are opposite, leading to this fortuitous near-cancellation of interference. Because of the unusual test-section configuration, further analysis is warranted, and the situation for larger-span test articles might be quite different.

Test Plan

There were 36 data runs accomplished, including longitudinal and lateral configurations with angles of attack ranging from $\alpha = -2$ to +20 deg, sideslip angles of $\beta = \pm 15$ deg, and canard and warp deflections δ_c and δ_w that covered the control operating range. Dynamic pressures of $0.85 \le Q \le 2.8$ psf ($40 \le Q \le 134$ Pa) were used to simulate the range of operating speeds, with the high end based on Wilbur's report.[15] Table 1 shows the test plan.

Longitudinal Results and Discussion

In Wilbur's 1901 paper, a reference is made to a test of cloth porosity to determine its effect on lifting capacity.[15] Two small experimental surfaces were evaluated: one that was "airproofed" and one that was left in its natural state. Wilbur reported no difference in their lifting powers; however, it is not clear if airproofing found its way to the 1901 machine. For the present test, two configurations were also examined to evaluate the effect of porosity on performance: untreated fabric and fabric that has been sealed with a starch-based paste.

Untreated Fabric

Runs 1–17 represent longitudinal runs with no sealer applied to the fabric, from which the baseline lift, drag, and pitching moment data were obtained. The untreated fabric weight was 3.8 oz/yd^2, and its permeability was determined to be 30.1 scfm (standard cubic feet/minute) at 0.5 in. H_2O differential pressure by the use of the Frazier Permeability Testing Machine. The basic variation of lift coefficient with angle of attack is plotted in Fig. 4, showing only slight influences of dynamic pressure on overall glider lift over the full dynamic pressure range from $Q = 0.85$ to 2.8 psf. At high angles of attack, the lift coefficient was reduced slightly with higher dynamic pressures due to leakage through the wing fabric and/or small camber change of the wing.

The zero-lift angle of attack was observed to be −1.2 deg, and the reference "straight line" lift coefficients are $C_{Lo} = 0.06$ and

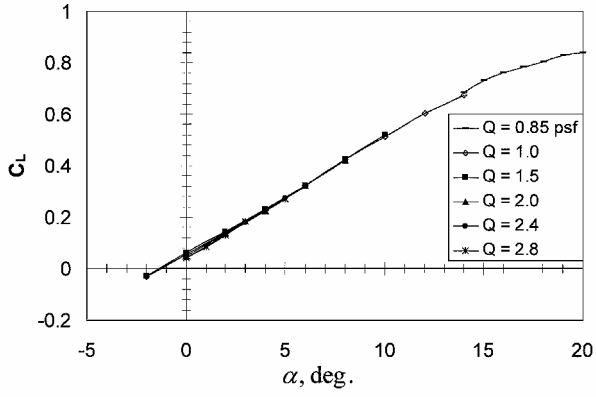

Fig. 4 Lift coefficient, 1901 glider.

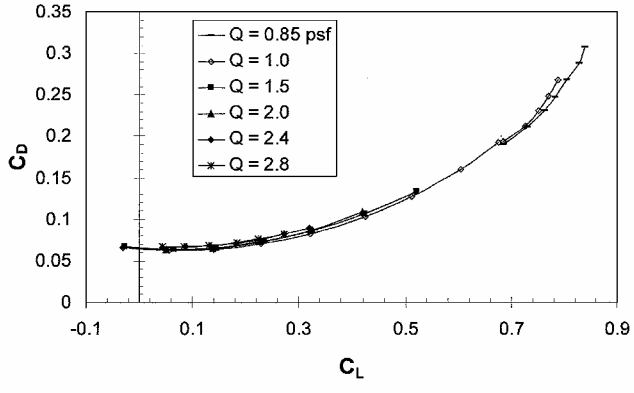

Fig. 5 Drag polar, 1901 glider.

$C_{L\alpha} = 0.045$/deg. The measured lift slope was in good agreement with a calculated value made by vortex lattice theory, with the model consisting of a single row of panels for the wings and canard. Degraded performance was due in part to the slot in the lower wing used to facilitate piloted takeoffs; the slot creates two smaller wings of aspect ratio 1.5.

The data in Fig. 4 show that the maximum lift coefficient was not yet achieved at the maximum 20-deg angle of attack tested. However, it is obvious that the maximum lift coefficient is close to the 20-deg limit, and it was estimated that $C_{L\,\max} = 0.85$ at $\alpha = 21$ deg, corresponding to a theoretical minimum flight speed of 20 mph (standard atmospheric conditions).

The variation in the aircraft baseline drag coefficient with angle of attack is shown in Fig. 5, over the range of tested dynamic pressures. Slight increases in drag occur at higher speeds, contrary an expected trend of lower drag as the Reynolds number increases from 1.2×10^6 to 2.2×10^6. This is likely the result of increased leakage rates between the lower and upper surfaces of each wing that would increase turbulent skin friction on both sides of the fabric. In addition, there is likely to be a slight difference in distortion of the wing fabric at increased airspeeds, and that too contributes to drag.

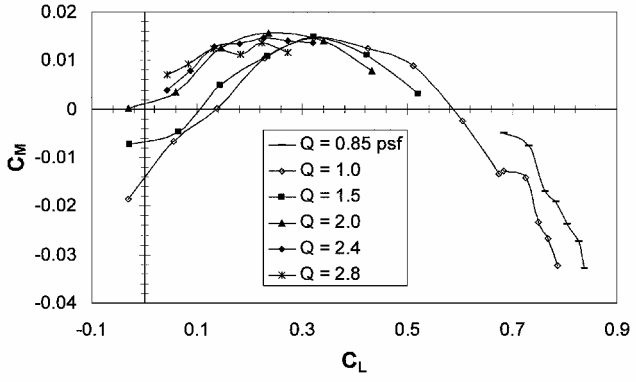

Fig. 6 Moment coefficient, 1901 glider.

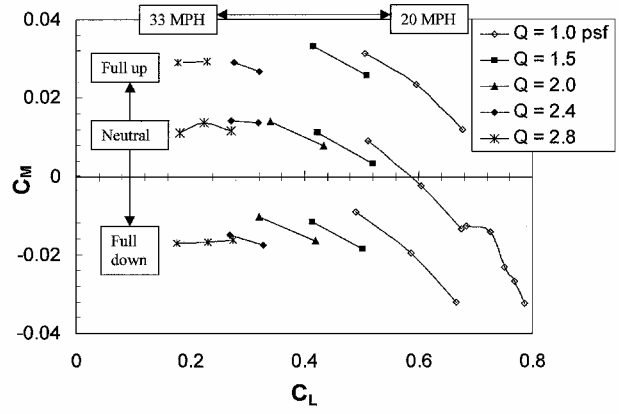

Fig. 7 Canard control power.

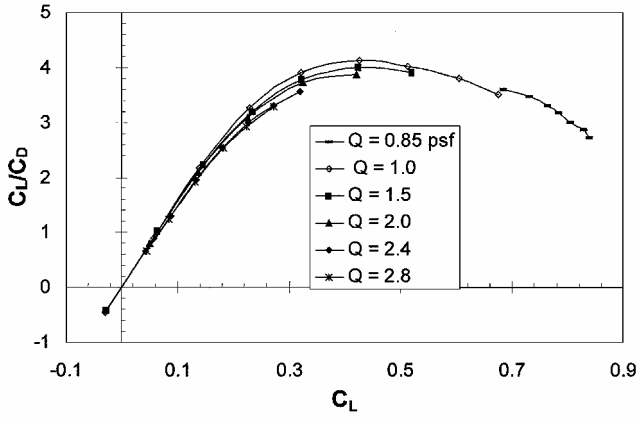

Fig. 8 *L/D*, 1901 glider.

Overall, drag was significantly higher than predicted, which was most likely due to the construction and shape of the wings. When the lifting surfaces were excluded, a parasitic drag study gave an equivalent flat plate area of 6.5 ft^2 (pilot, struts, trussing posts, and wires). The drag of the lifting surfaces has not been included because their profile drag exhibits linear and quadratic dependency to C_L.

The lack of a fabric fairing, or cuff, around the bottom wing leading-edge spar contributed to an increase in the profile drag of the lower wing. The triangular spar has a sharp rear edge and vertical rear surface that causes separation and significant base drag to develop. The top wing had a small strip of fabric bridging the bottom of the leading-edge spar to the rest of the wing, which reduced, but did not eliminate, this source of drag. Other profile drag contributors included the top-mounted rear spars that are not faired and the wake caused by the interaction between the pilot (dummy) and the lower wing slot. Note that tufting of the top and bottom wings revealed no attached flow beyond 50% of the chord at angles of attack greater than 4 deg.

The variation in pitching moment with lift coefficient is shown in Fig. 6, referenced at the c.g. of 19.9 in. aft of the leading edge on the bottom wing, under the assumption of a nominal pilot position. The hump shape is partly caused by the biplane/canard configuration and partly from the c.p., x_{CP}, shift on the relatively inefficient airfoil. Separated flow near the front of the airfoil will cause x_{CP} to shift aft as the angle of attack is increased, causing a more negative pitching moment. The static margin (SM), defined by $\mathrm{SM} = (x_{\mathrm{np}} - x_{\mathrm{c.g.}})/\bar{c}$ at trimmed, level flight conditions, increases from a nearly neutral value at $Q = 2.8$ psf to a high value of 25% at $Q = 1.1$ psf. When the dynamic pressure is increased, the moment curve shifts to the left, and this is probably the result of two factors:

1) Drag on the trussing lines (that hold the top wing in reflex) will increase top wing reflex as dynamic pressure increases.

2) Cable tension variations will cause the wings to take on new equilibrium angles of attack as the glider static weight is lifted from the balance with increasing dynamic pressure.

In addition to the moment curve shifting left, the moment values decreased for $\alpha > 6$ deg when the dynamic pressure was increased. This was most likely caused by a deformation of the wings as they became more heavily loaded, with higher dynamic pressure causing an increase in wing camber.

Canard effectiveness is shown in Fig. 7, for only those portions of the test data corresponding to the trim flight speeds at a load factor $n_z = 1$. With standard atmospheric conditions, trim control is available from 21 mph to speeds higher than the Wrights recorded (36 mph). The aircraft can not be flown without shifting the c.g. at speeds slower than 21 mph because the canard has reached its full pitch-up travel, and the pitch stability has increased to SM = 25%. It is certainly likely that the pilot combined canard inputs with a change in his body position to augment longitudinal control, with stability decreasing by $\Delta\mathrm{SM}/\Delta\text{pilot c.g.} = -0.76\%/\text{in.}$ and trim moment coefficient increasing by $\Delta C_m/\Delta\text{pilot c.g.} = 0.0056/\text{in.}$ as the pilot moved aft.

Because canard control involves changing the camber, deflection is crudely defined by the angle resulting from a measurement between the trailing edge and the leading edge. Full deflection is ± 5.3 deg, which results in an average $C_{m\,\delta c} = 0.0040/\text{deg}$.

Figure 8 shows the measured L/D of the aircraft, outside of ground effect. A maximum $L/D = 3.9$ was measured at a trim flight speed of 28 mph ($C_L = 0.42$ and $Q = 2.0$ psf under standard conditions), considerably less than what was observed 100 years earlier when the Wrights consistently reported glide ratios and kited L/D measurements of about 6. By the use of the same vortex lattice model that was used to estimate lift, induced drag reduction in ground effect was estimated to be from $C_{D\,\mathrm{ind}} = 0.18C_L^2$ to $0.14C_L^2$ for a 3-ft flight altitude. This increases the L/D to 4.2, which is a marginal increase, mainly due to the large values of parasitic and profile drag that have constant, linear, and quadratic terms in C_L. Because much of the gliding performed by the Wrights was on a hill with a 10 deg slope,[9] a combination of dynamic soaring, vertical wind vector strength, and a tighter, less porous fabric weave could explain their substantially higher lift-to-drag performance. Figure 8 also shows that the low aspect ratio design provides a reduction in L/D at high C_L that will most likely get the pilot on the ground before a stall develops.

As a note on the wind-tunnel measured performance being less than that reported by the Wrights, a fundamental problem in the testing of early wood, fabric, and wire aircraft is revealed that certainly played a role in the Wrights' own aeronautical research. These aircraft are inherently variable, and if quantifiable data are desired, then documentation of in-flight geometry, as well as the recording of accurate speed, angle of attack, and wind velocity, would be necessary. Limited instrumentation at the Outer Banks did not allow such detailed measurements, and other environmental factors such as moisture content that affects fabric permeability were not recorded. In addition, the lack of standard terminology and geometrical references would result in the need to transform information from aircraft to aircraft, causing yet another potential source of error. Without fully understanding the effects of aspect ratio and camber

until they returned to Dayton, the Wrights found the performance of the 1901 glider disappointing.

In all, the data accessed by the Wrights, as well as their own measured data, showed undocumented uncertainty and an omission of critical parameters that provided them the incentive to build a wind tunnel and conduct basic airfoil and wing design research. The return from Kitty Hawk in 1901 was a significant turning point in the progress of aviation in that data would now, for the first time, be repeatable.

Airproofed Fabric

Sealing the wings with a starch-based paste gave performance closer to that reported by the Wrights. Runs 32–36 are the basic longitudinal runs for this condition. Figures 9–11 show the measured

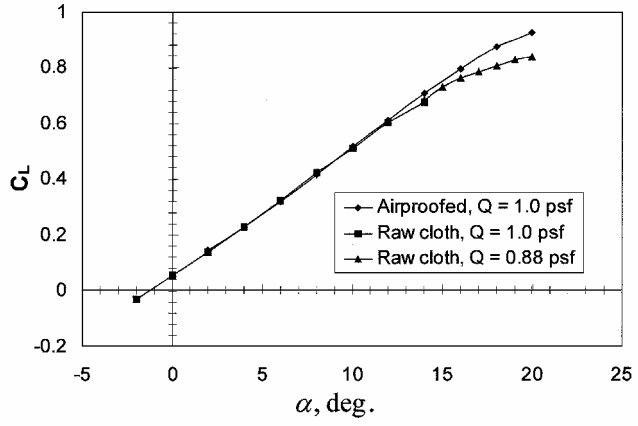

Fig. 9 Lift coefficient, with airproofing.

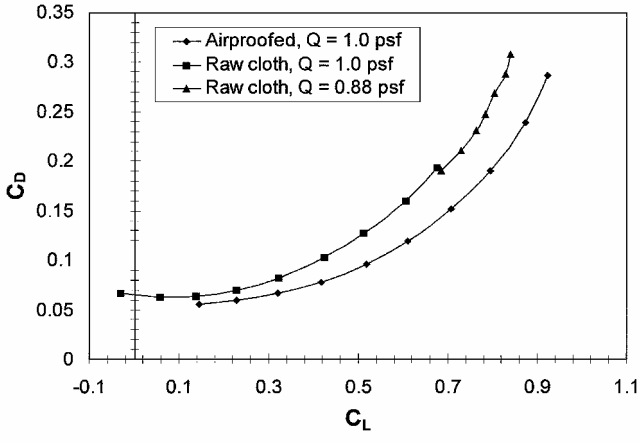

Fig. 10 Drag polar, with airproofing.

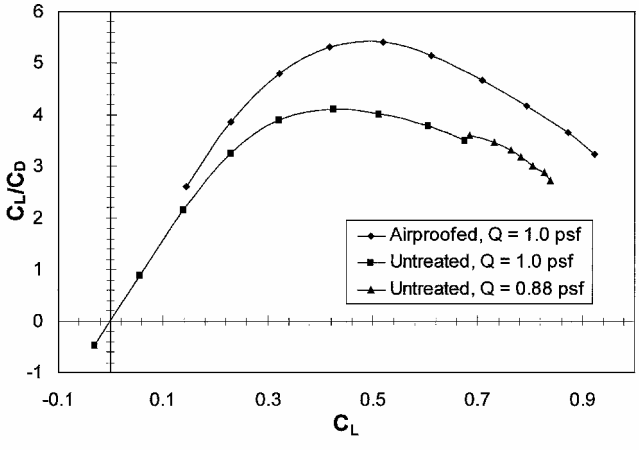

Fig. 11 *L/D*, with airproofing.

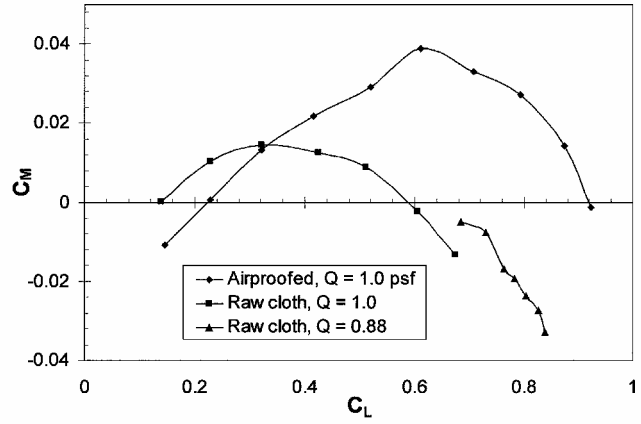

Fig. 12 Moment polar with airproofing, 1901 glider.

lift, drag, and L/D. The maximum L/D for a dynamic pressure of $Q = 1.0$ psf increases from 4.1 to 5.2. Note that this dynamic pressure is not sufficient to sustain unaccelerated, level flight at the maximum L/D, but this, nevertheless, serves as a useful example of the benefit associated with airproofing. Because of the decreased drag with airproofing, ground effect will account for a larger percentage of drag reduction, resulting in an estimated optimal $L/D = 5.8$ for trimmed, level flight at $C_{L\,\mathrm{trim}} = 0.50$.

The application of the paste treatment reduces permeability, tightens the fabric, adds mass, and increases the surface roughness by adding thickness to stray fibers in the cloth. With the exception of the increased roughness, all other factors would reduce drag because bottom-to-top air leakage is suspected of increasing turbulent skin friction, and the fluttering of the cloth is suspected of dissipating energy into the freestream. No quantitative analysis on permeability was performed after sealing because the aircraft was loaned for display at a museum immediately after testing.

If the Wrights used a tighter, less porous weave in their 1901 glider than what was used in the reproduction glider, it is possible that they achieved their reported performance without airproofing. This test, however, clearly shows that drag is reduced when a sealer is applied to the raw fabric through a combination of reduced porosity, increased membrane tension, and increased mass density.

In addition to reducing drag, the application of the airproofing has an effect on the pitching moment. Figure 12 shows the moment polar when the surfaces have been treated, indicating that the aircraft is now about 9% unstable up to $C_L = 0.63$. As will be shown in the next section, this does not make the aircraft uncontrollable; however, the pilot will have to move forward to counteract the increased positive moment and remain on the controls at all times. The canard control power remains the same in this condition.

The moment curve shift is most likely due to the delayed separation resulting from reduced leakage in the airproofed fabric that increases the effectiveness of the reflexed airfoil, causing a positive pitching moment increment. Another effect of the airproofing is the improved shape stability of the leading edge, which, again, delays separation beyond the original, untreated condition.

Lateral Results and Discussion

Runs 18–31 represent the lateral runs, including wing warp and sideslip. Figure 13 shows the roll effectiveness $C_{l\delta w}$ for $\frac{1}{3}$, $\frac{2}{3}$, and full warp deflection of $\delta_w = 4.3$ deg (measured at the wing tip), averaged over a range of angles of attack (AOA) from 2 to 11 deg. Roll damping was determined to be $C_{lp} = -0.33$ when a warped vortex lattice model was used, as was the case with a straight model that gave spanwise $C_{L\alpha}$ to be used in a numerical integration scheme. The resulting roll equation for a step input of full warp deflection is

$$\Delta p = 0.12(1 - e^{-8.2t}) \tag{3}$$

The theoretical steady-state roll rate is 7 deg/s, with $pb/2u = 0.032$ rad, compared to an acceptable range of 0.05–0.10 rad

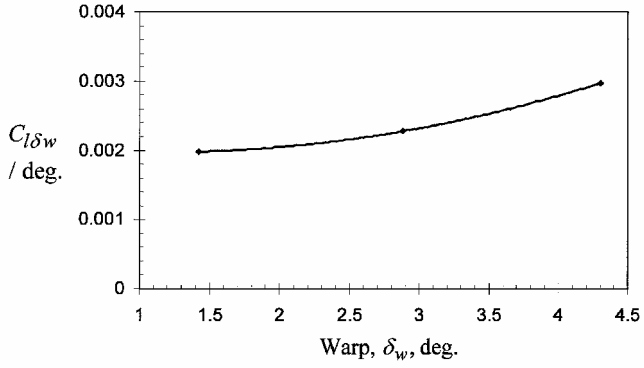

Fig. 13 Average warp effectiveness, $Q = 2.0$ psf.

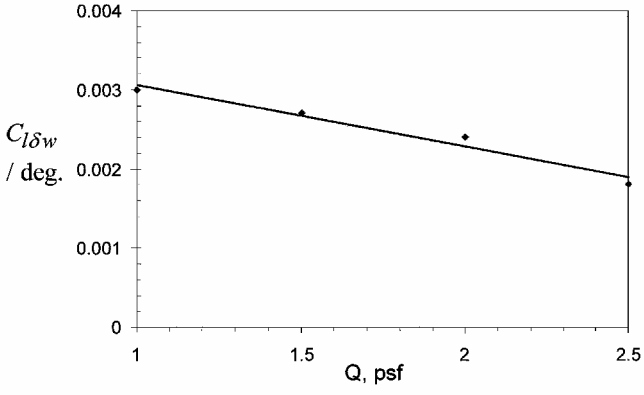

Fig. 14 Reduction in roll power as a function of dynamic pressure.

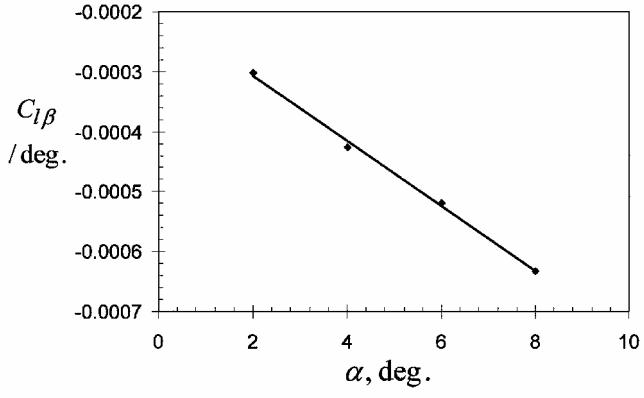

Fig. 15 Dihedral effect, $Q = 2.0$ psf.

(Ref. 15) for most aircraft. As will be shown later, adverse yaw prevents a steady roll rate from being developed in this aircraft.

Figure 14 shows the reduction in $C_{l\delta w}$ as a function of dynamic pressure. Because the wing warping lines are not steel, but braided cotton cord, the wing tends to untwist under higher loads, effectively decreasing the roll coefficient. Some of this effect can also be attributed to flexibility in the ribs.

Adverse yaw was determined to be $C_{n\delta w} = -2.8 \times 10^{-4}$/deg at a trim lift coefficient of $C_L = 0.42$, with little effect attributed to dynamic pressure. Additionally, the glider showed only slight yaw stability due to the lack of vertically oriented surfaces. Accurate measurements of $C_{n\beta}$ were not possible due to the resolution of the external balance, but the value is likely to be very small due to a lack of vertical surfaces.

The glider demonstrated dihedral stability, as shown in Fig. 15. This is most likely caused by the disturbance of flow over the bottom, downwind wing due to an upwash through the central slot. The location of the pilot also would enhance the dihedral effect, increasing the AOA on the upwind wing and decreasing the angle on the downwind wing. In 1902, the Wrights identified dihedral stability as a control problem for a ground-effect glider, where a side gust would roll the aircraft away from the gust, causing the downwind wingtip to make contact with the ground. As noted in the 1903 Flyer configuration, anhedral was built into some of the later designs to keep the airplane better aligned with the nominal freestream velocity.

Dynamic Simulation

Longitudinal

A dynamic simulation using Simulink™ was performed to examine the flight handling qualities of the 1901 glider. This information is useful in understanding how the Wright brothers' subsequent designs evolved as a result of their test program. Two cases were examined: one based on the untreated cloth data and one based on the airproofed condition.

The dynamic model is based on linear derivatives for u, w, q, and θ at around the best L/D speed of 28 mph, corresponding to $Q = 2.0$ psf (standard conditions). Figure 16 shows the stick-fixed gust response of the untreated glider when subjected to a one-half-sine vertical pulse of magnitude 1 ft/s. The phugoid mode is evident in the Fig. 16, with a period of $T = 8.4$ s and a damping ratio of $\zeta = 0.096$. The short period mode has a period of $T = 1.4$ s and a damping ratio of $\zeta = 0.67$.

When the wings are airproofed, simulation must now include the pilot in the loop because the aircraft has become unstable. With a canard response of $\delta_c = -0.22\theta - 0.10q$ with a 0.2-s delay, a 95% settling time of 4 s was achieved for the same 1 ft/s gust. This is a worse-case simulation that does not reduce the instability when the pilot moves forward, which would most likely be the case to achieve trimmed flight.

Lateral

In this simulation, a linear model was again used based on the derivatives measured about the trim flight speed of 28 mph, and state variables β, p, r, and ϕ were chosen to describe the motion. The Wright 1901 glider lacked any vertical surfaces, resulting in an inability to counteract adverse yaw, which gave the operator a unique experience in lateral control. Figure 17 shows a full-deflection, one-half-sine pulse of right warp to initiate a right-hand turn. However, soon after the glider begins a turn to the right, adverse yaw steers the glider to the left, and the dihedral effect, combined with roll due to yaw rate, places the aircraft into a steady left-hand turn. It appears from these results that the warping control worked effectively in reverse, where a warp to the right resulted in a left-hand turn, and warp to the left resulted in a right-hand turn. The warping system was effective in turning the glider, but only from the standpoint that it functioned as a differential drag device.

The Wrights recognized this incongruity and wrote about it: "We proved that our machine does not turn (i.e., circle) toward the lowest wing under all circumstances, a very unlooked for result and

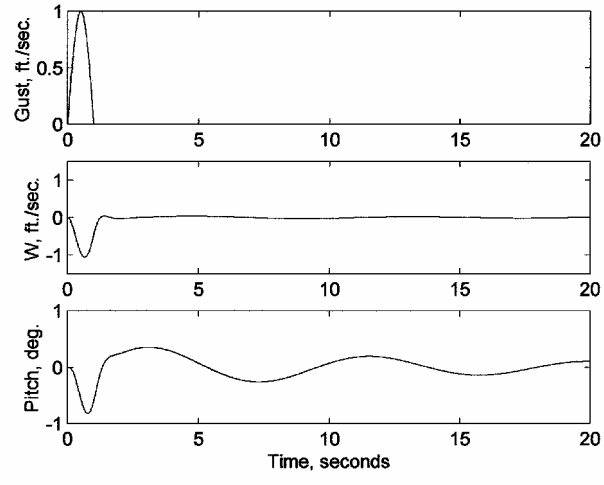

Fig. 16 Stick-fixed gust response, one-half-sine pulse gust input.

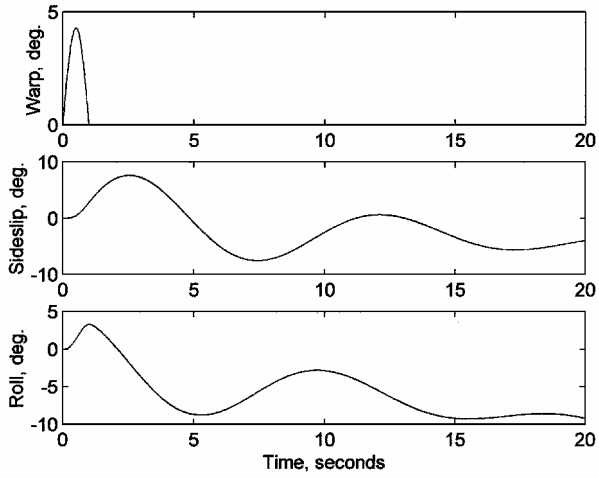

Fig. 17 Roll response, one-half-sine pulse warp input.

one which completely upsets our theories as to the causes which produce the turning to right or left."[16] Jakab notes that in initial tests of the 1901 glider's lateral control, a left-hand turn would begin normally (roll in the direction of warp), "but partway into the turn, the glider reversed direction and began to turn about the high wing, to the right."[6] The lateral control conundrum was solved in 1902, when a movable rudder was added their machine, resulting in a modern, three-axis control system. The poles of this system consist of a fast roll mode pole, $\lambda_1 = -8.24$, a slow unstable divergent pole, $\lambda_2 = 0.060$, and the oscillatory poles described by $\lambda_{3,4} = -0.11 \pm 0.65i$.

Conclusions

Many authorities have referred to the Wright 1901 gliding experiments as marginally successful, but the lessons learned from these flights became the impetus to address the problems of flight with renewed vigor. On returning to Dayton, they constructed a wind tunnel and systematically tested airfoils to determine corrections to the Lilienthal tables that would resolve the discrepancies observed in flight tests. The lateral handling problems were solved with the addition of a rudder to the 1902 machine. Finally, measured drag on the 1901 glider was higher than they desired, and so subsequent aircraft were cleaned up to improve the glide ratio.

The test results from this program showed that the Wright 1901 reproduction glider had sufficient drag in the raw fabric condition to preclude flight performance that matched the recorded performance in 1901. The low L/D value of 3.9 was boosted to 4.2 when in ground effect at a flight altitude of 3 ft, but this was still well below the recorded L/D value of 6 during many of the original piloted and kited flight tests. Only with an airproofing treatment of the cloth did the L/D rise to a value of 5.8, which was close to what was originally reported. It appears that, although it is still uncertain if the Wrights used a treatment to their cloth, the evidence indicates that the cloth used for this test was too porous to match the flight-test results. This finding has also provided insight into likely problems that the Wrights' had in comparing their flight-test results with published data. Flexible, fabric-covered aircraft are difficult to quantify under the best of conditions, let alone when the variability of the natural test environment is also factored in.

The glider was longitudinally stable in the raw fabric condition and unstable at trim conditions when the cloth was airproofed. This did not present a problem in simulations because the slow unstable pole gives the pilot time to react.

The use of wing warping to effect lateral control was effective, although not in the way the Wrights intended. Both in test and documentation from the flights 100 years ago, the 1901 glider experienced significant adverse yaw that resulted in opposite direction turns from the wing warping input. Small control inputs from the operator and some flight experience were undoubtedly required to master the lateral control system.

Results of this test showed that the evolution of Wright aircraft designs were not as straight forward as one might imagine. The lateral control anomaly was a result of adverse yaw and dihedral stability acting against the wing warping command, with neither phenomenon having been identified at the time of the experiments. Adding a vertical surface in 1902 to reduce the adverse yaw tendency did not solve the turning problem until the surface became a movable rudder, used mainly to arrest roll rate into the low wing.

The quest to master three-axis control was the result of iteratively solving the problems that developed with every new glider design. Things that worked, such as the canard control effectiveness, were retained and changed little over the years leading to 1903. The addition of the movable rudder and wing anhedral in 1902 were the product of observations and intuition that resulted in adequate, predicable lateral handling qualities necessary for powered flight. The 1901 glider was critical in providing the Wrights with many important observations needed to solve the overall problem of powered flight, and, in many ways, 2002 is the 100th anniversary of the beginning of the systematic approach to aeronautical engineering.

Acknowledgments

The authors would like to acknowledge the support of NASA Langley Research Center, under Education Cooperative Agreement NCC-1-379, for supporting portions of this research. The Wright Experience™ is also acknowledged for providing the reproduction 1901 glider, along with technical support required during the test.

References

[1]Jex, H. R., Grimm, R., Latz, J., and Hange, C., "Full-Scale 1903 Wright Flyer Wind Tunnel Test Results from the NASA Ames Research Center," AIAA Paper 2000-0512, Jan. 2000.

[2]Bettes, W. H., and Culick, F. E. C., "Report on Wind Tunnel Tests of a 1/6-Scale Model of the 1903 Wright Flyer Airplane," Guggenheim Aeronautical Lab., California Inst. of Technology, GALCIT Rept. 1034, Pasadena, CA, 1982.

[3]Jex, H. R., Magdaleno, R. E., and Lee, D., "Virtual Reality Simulation of the '03 Wright Flyer Using Full Scale Test Data," AIAA Paper 2000-4088, Aug. 2000.

[4]Crouch, T., *The Bishop's Boys*, W. W. Norton, New York, 1989, p. 173.

[5]Wright, W., "Some Aeronautical Experiments," *Flying*, March 1902, p. 93.

[6]Jakab, P. L., *Visions of a Flying Machine, The Wright Brothers and the Process of Invention*, Smithsonian Inst. Press, Washington, DC, 1990, pp. 101–113.

[7]Culick, F. E. C., "What the Wright Brothers Did and Did Not Understand About Flight Mechanics-In Modern Terms," AIAA Paper 2001-3385, July 2001.

[8]Wright, W., "Some Aeronautical Experiments," *Flying*, June 1902, p. 140.

[9]McFarland, M. W., *The Papers of Wilbur and Orville Wright*, Vol, 1, reprint, Ayer, Salem, NH, 1990, pp. 80–89.

[10]Wright, W., "Some Aeronautical Experiments," *Flying*, Sept. 1902, p. 189.

[11]Miley, S. J., Ash, R. L., Hyde, K., Landman, D., and Sparks, A., "Propellers Performance Tests of Wright Brothers Bent-End Propellers," *AIAA Journal*, Vol. 39, No. 2, 2002, pp. 234–241.

[12]Fitts, T. S., and Britcher, C. P., "Refurbishment and Recalibration of the External Balance at the Langley Full-Scale Tunnel (LFST)," Rept. LFST 02-01, NASA Langley Research Center, Hamilton, VA, May 2002.

[13]"The Assessment of Experimental Uncertainty with Application to Wind-Tunnel Testing," AIAA Standards Series S-071A-1999, 1999.

[14]Barlow, J. B., Rae, W. H., and Pope, A., *Low Speed Wind Tunnel Testing*, 3rd ed., John Wiley and Sons, New York, NY, 1999.

[15]Wright, W., "Some Aeronautical Experiments," *Flying*, Jan. 1903, p. 226, Chaps. 9 and 10.

[16]McCormick, B. W., *Aerodynamics, Aeronautics, and Flight Mechanics*, Wiley, New York, 1995, p. 527.